

Supporting Information

Development of intense yellow color BiVO₄/ZrO₂ composite coating for anticorrosive multifunctional cool roof

A. H. Riyas,¹ C.V. Geethanjali,¹ Liya Johnson,¹ Liju Elias,¹ A.M.A. Henaish,² Aslam Hossain,³
S. M. A. Shibli^{1,4*}

¹Department of Chemistry, University of Kerala, Karyavattom campus, Thiruvananthapuram,
Kerala – 695 581, India

²NANOTECH Center, Ural Federal University, Ekaterinburg 620002, Russia.

³Smart Materials Research Institute, Southern Federal University, Sladkova 178/24, 344090,
Rostov-on-Don, Russia

⁴Centre for Renewable Energy and Materials, University of Kerala, Kariavattom Campus,
Thiruvananthapuram, Kerala, 695 581, India

*Corresponding Author: S.M.A. Shibli Ph: +91 8547067230, E. mail: smashibli@yahoo.com

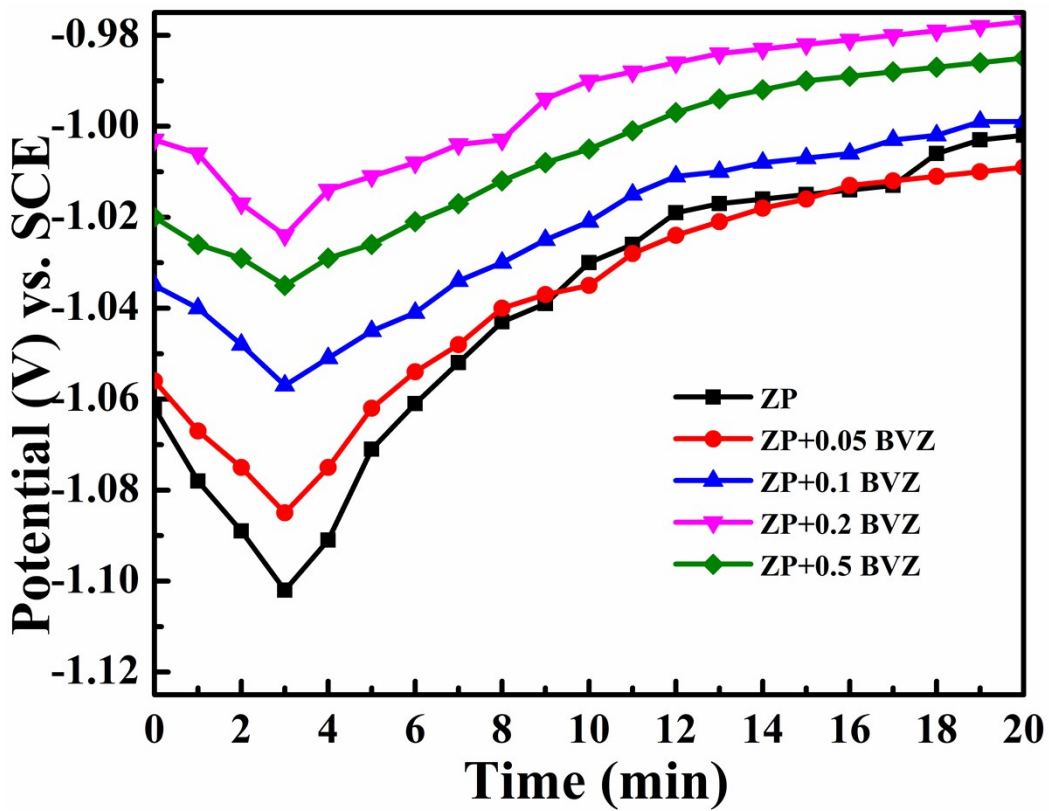


Fig. S1. The trend of potential-time curves obtained during the zinc phosphating process of galvanized steel in the presence and absence of BVZ composites

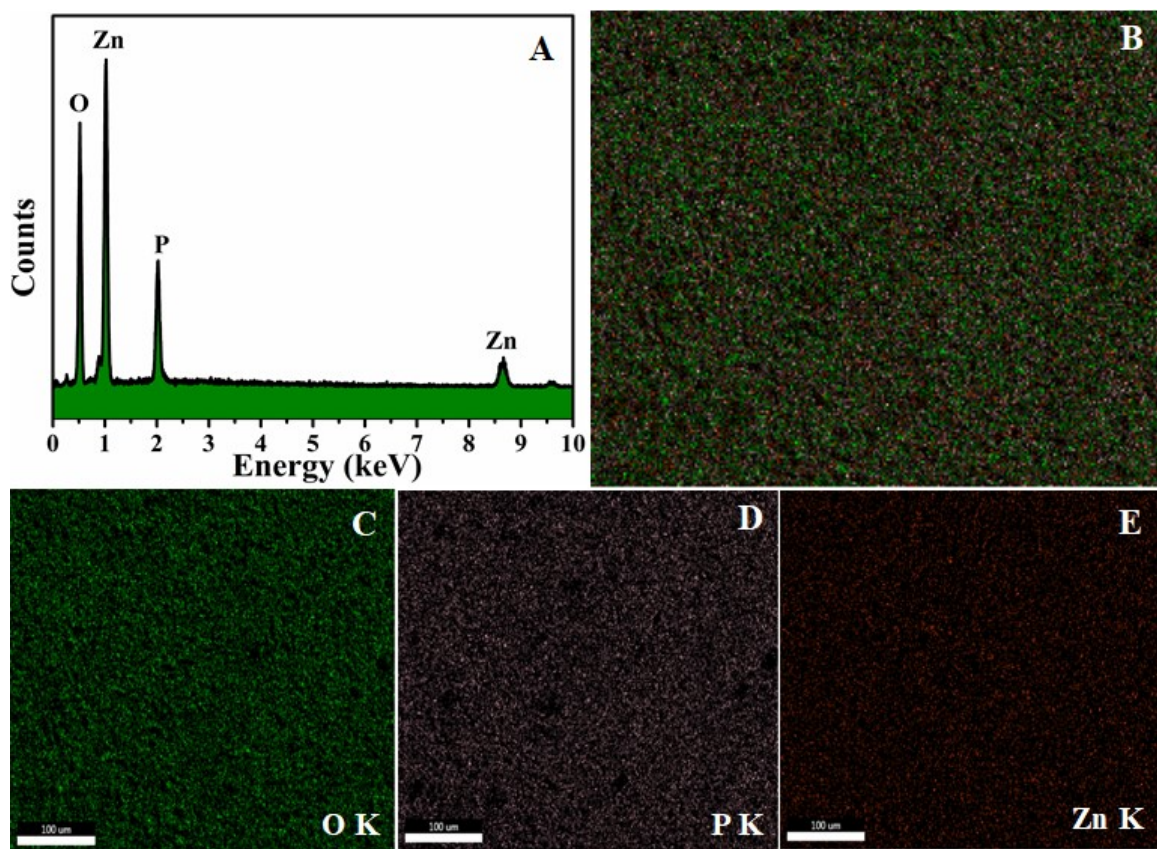


Fig. S2. (A) EDS spectrum and EDS elemental mapping spectrum of zinc phosphate coating developed from the bath in the absence of BVZ composite; (B) EDS layered image, (C) O K, (D) P K and (E) Zn K

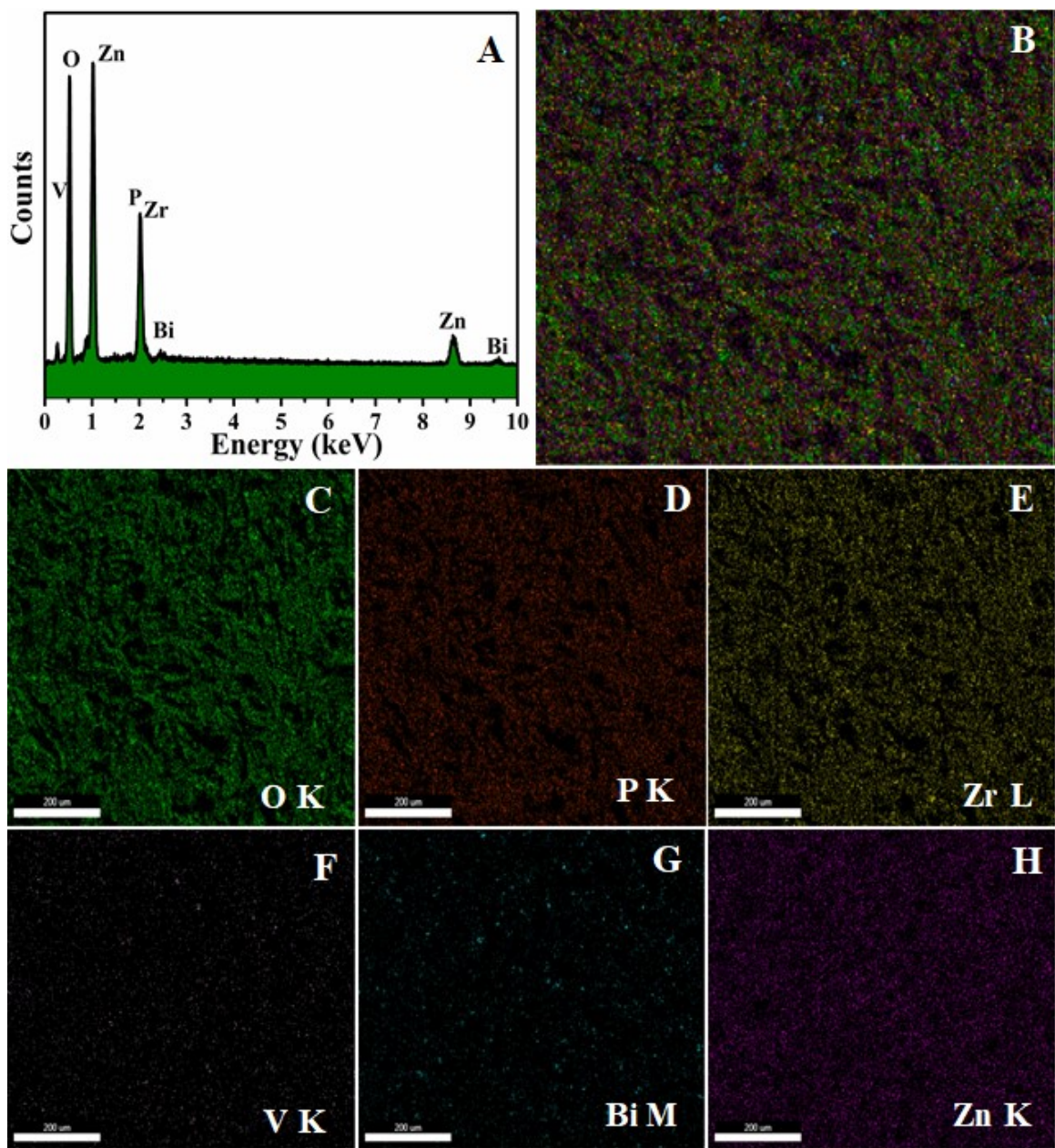


Fig. S3. (A) EDS spectrum and EDS elemental mapping spectra of zinc phosphate coating developed from the bath containing 0.05 wt.% of BVZ composite; (B) EDS layered image, (C) O K, (D) P K, (E) Zr L, (F) V K, (G) Bi M and (H) Zn K

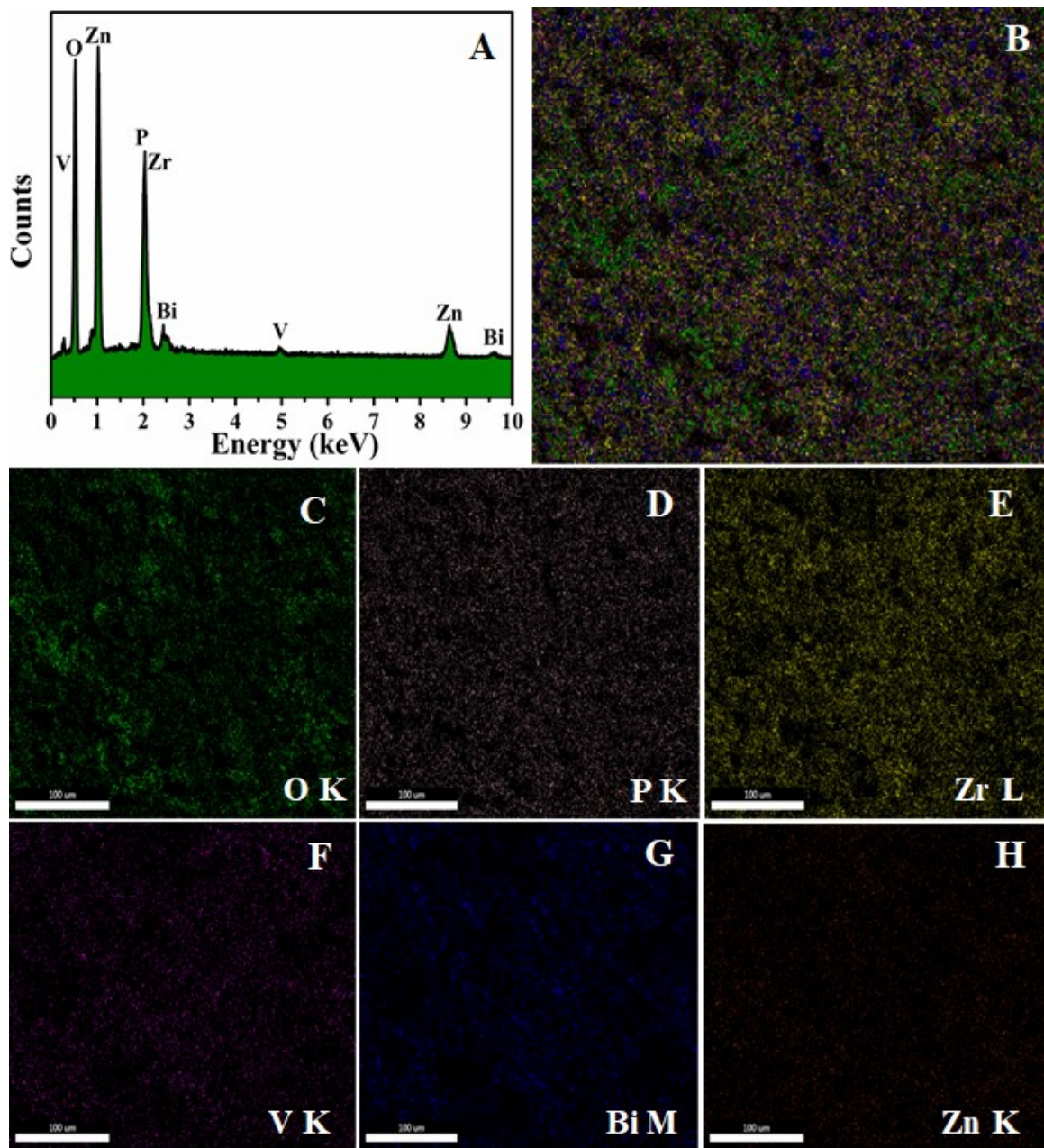


Fig. S4. (A) EDS spectrum and EDS elemental mapping spectra of zinc phosphate coating developed from the bath containing 0.1 wt.% of BVZ composite; (B) EDS layered image, (C) O K, (D) P K, (E) Zr L, (F) V K, (G) Bi M and (F) Zn K

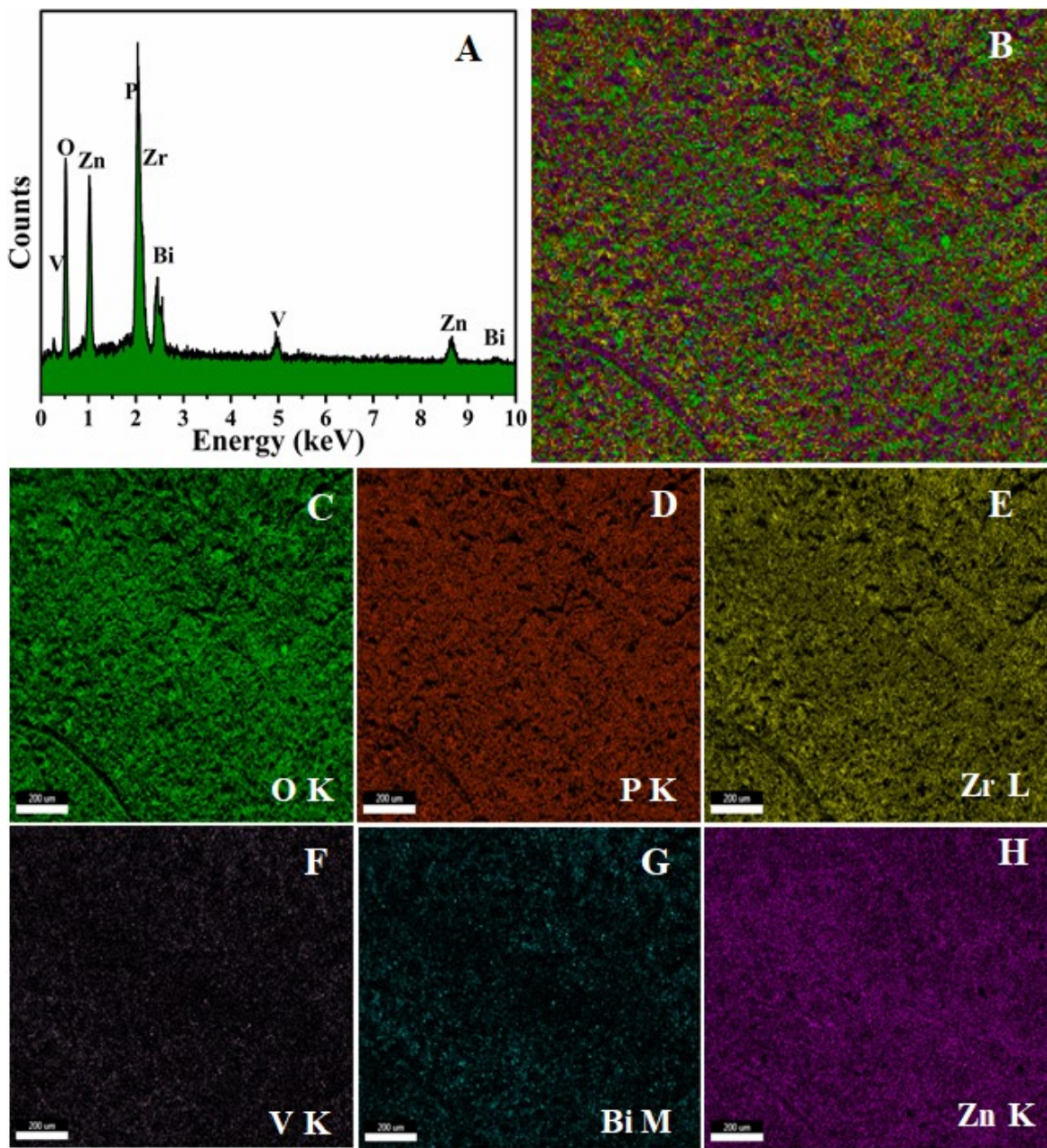


Fig. S5. (A) EDS spectrum and EDS elemental mapping spectra of zinc phosphate coating developed from the bath containing 0.2 wt.% of BVZ composite; (B) EDS layered image, (C) O K, (D) P K, (E) Zr L, (F) V K, (G) Bi M and (F) Zn K

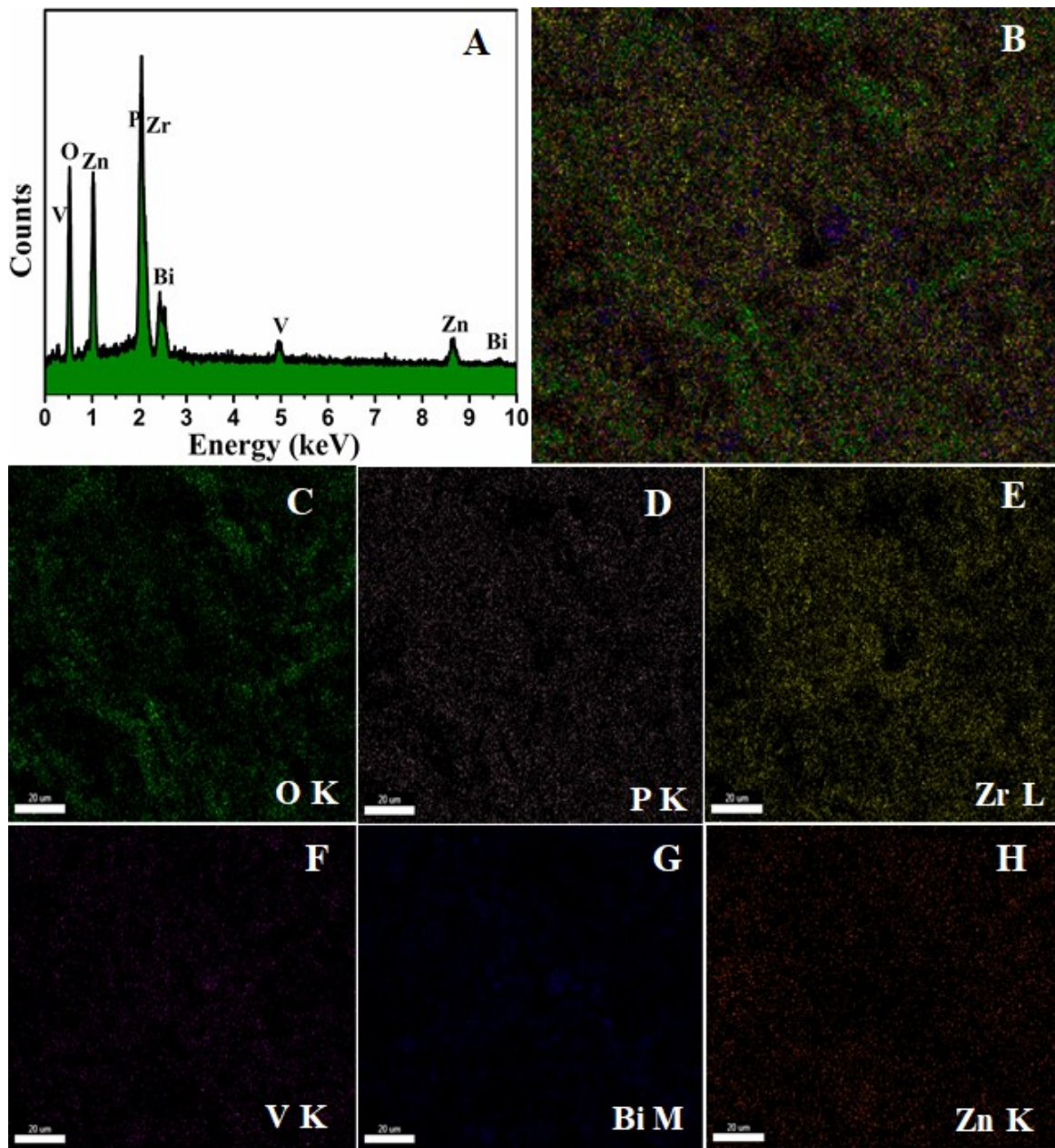


Fig. S6. (A) EDS spectrum and EDS elemental mapping spectra of zinc phosphate coating developed from the bath containing 0.5 wt.% of BVZ composite; (B) EDS layered image, (C) O K, (D) P K, (E) Zr L, (F) V K, (G) Bi M and (F) Zn K

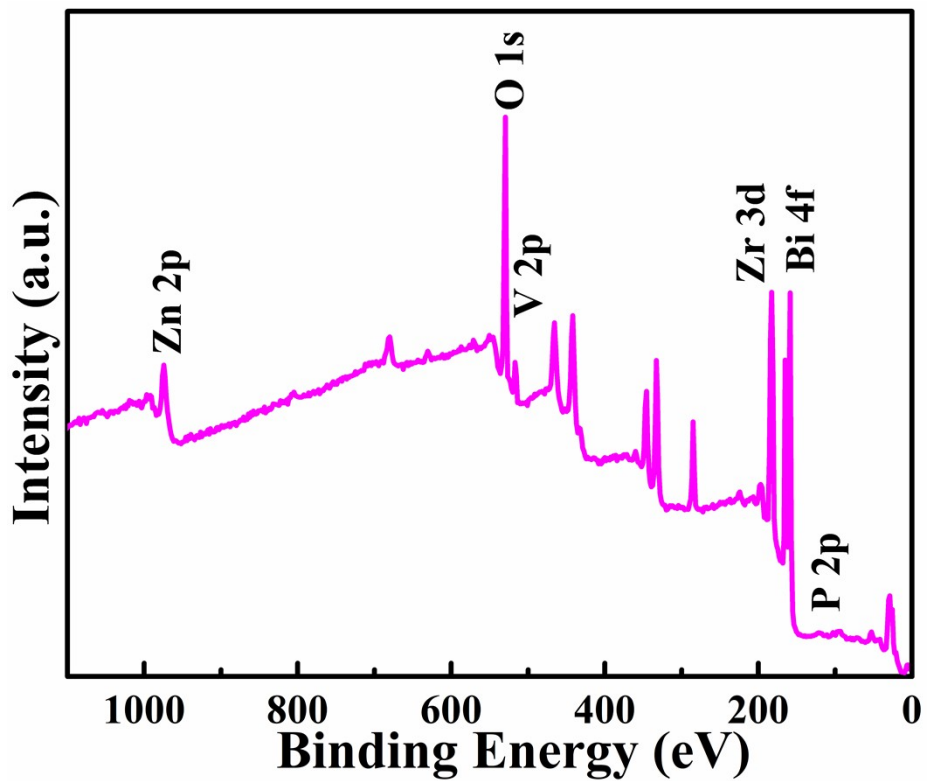


Fig. S7. XPS survey spectrum of zinc phosphate coatings developed from the bath containing BVZ composite

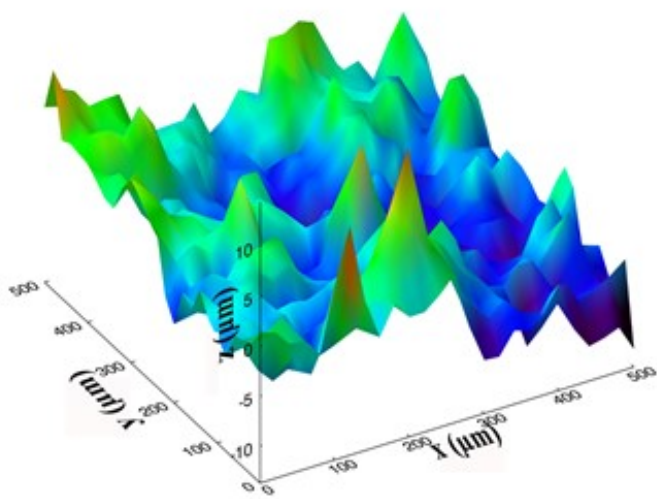


Fig. S8. OSP 3D images of bare zinc phosphate coatings

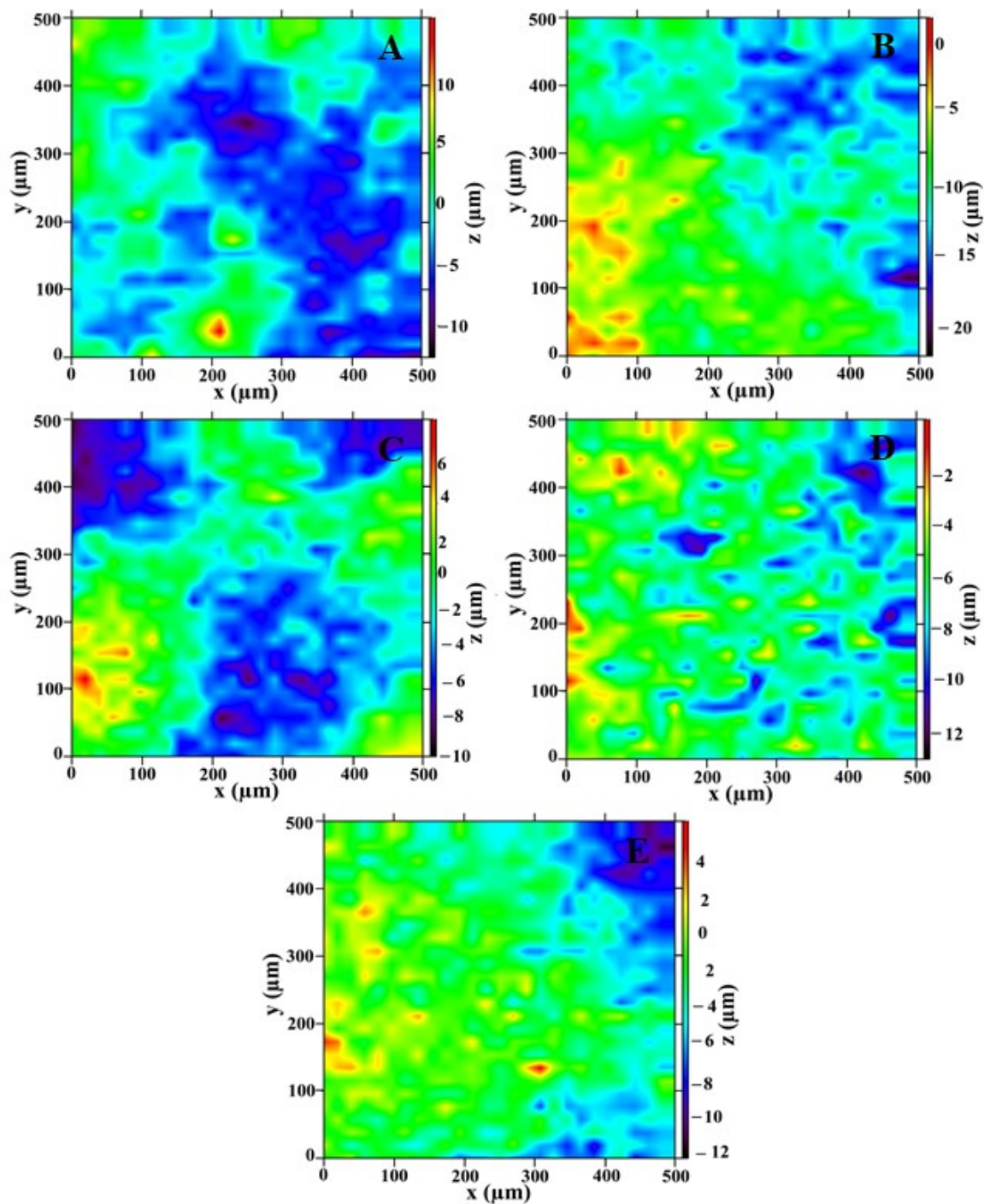


Fig. S9. OSP 2D images of zinc phosphate coatings developed from the bath containing different compositions of BVZ composite: (A) 0 wt.%, (B) 0.05 wt.%, (C) 0.1 wt.%, (D) 0.2 wt.% and (E) 0.5 wt.%

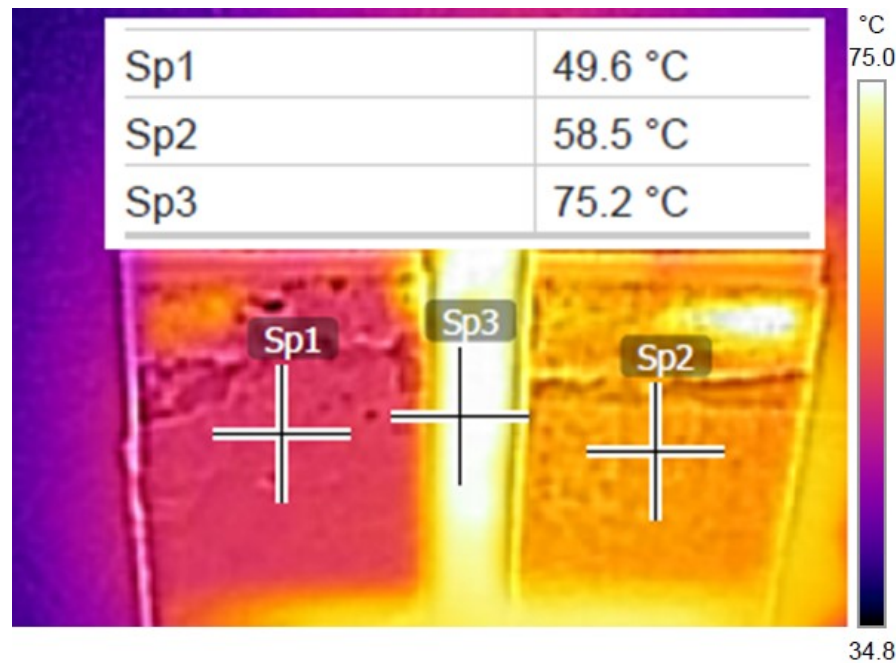


Fig. S10. FLIR thermal image of bare zinc phosphate coatings with and without BVZ composite (Sp1 – Temperature of zinc phosphate coating with BVZ composite, Sp2 – Temperature of zinc phosphate coating without BVZ composite, and Sp3 – Temperature of hot plate region)

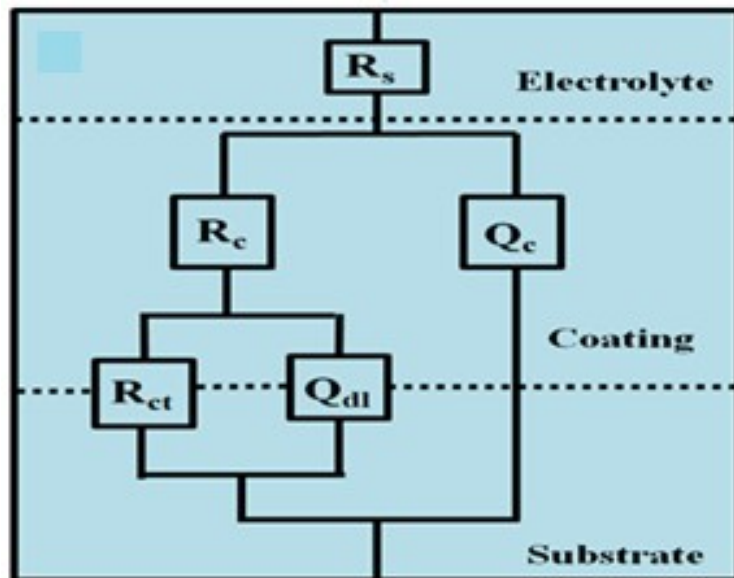


Fig. S11 equivalent circuit of of BVZ composite zinc phosphate coatings

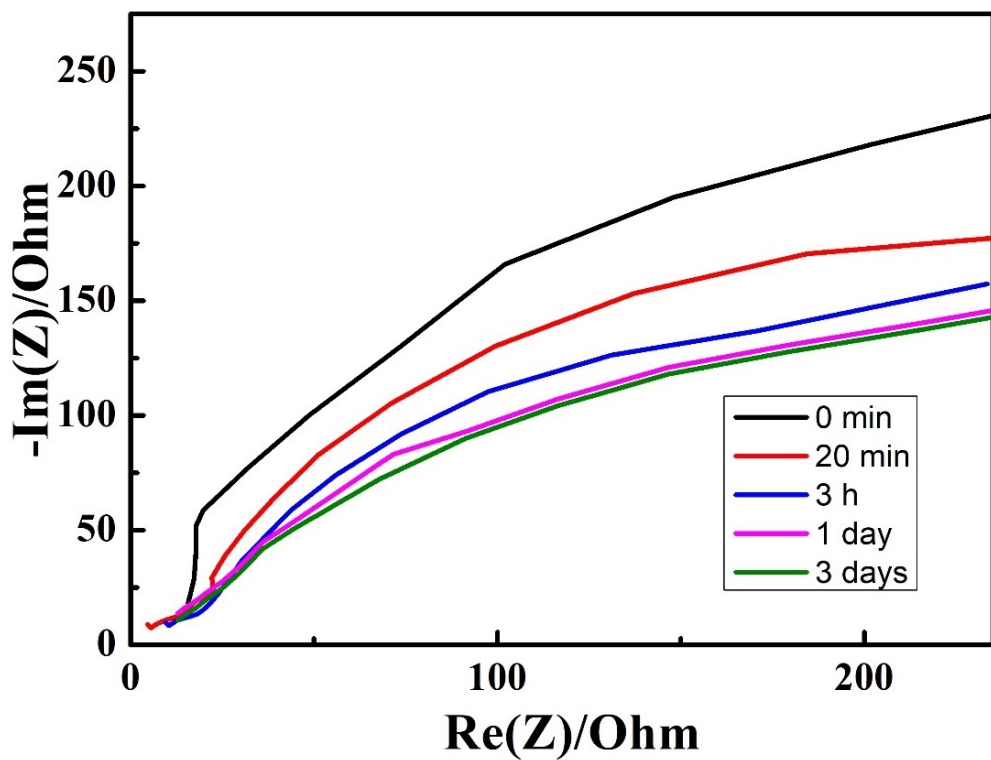


Fig. S12. Nyquist plots of 0.2 wt.% BVZ coating after 0 min, 20 min, 3 h, 1 day and 3 days immersion in 3.5 wt.% NaCl solution.

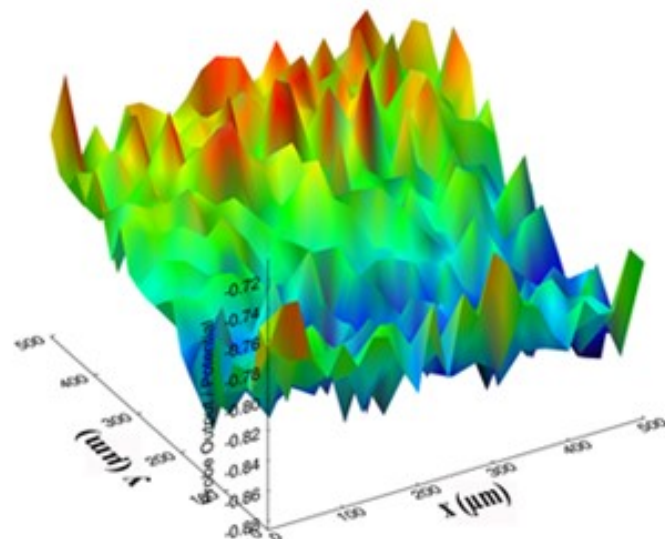


Fig. S13 3D SKPM images of (A) 0 wt.%,

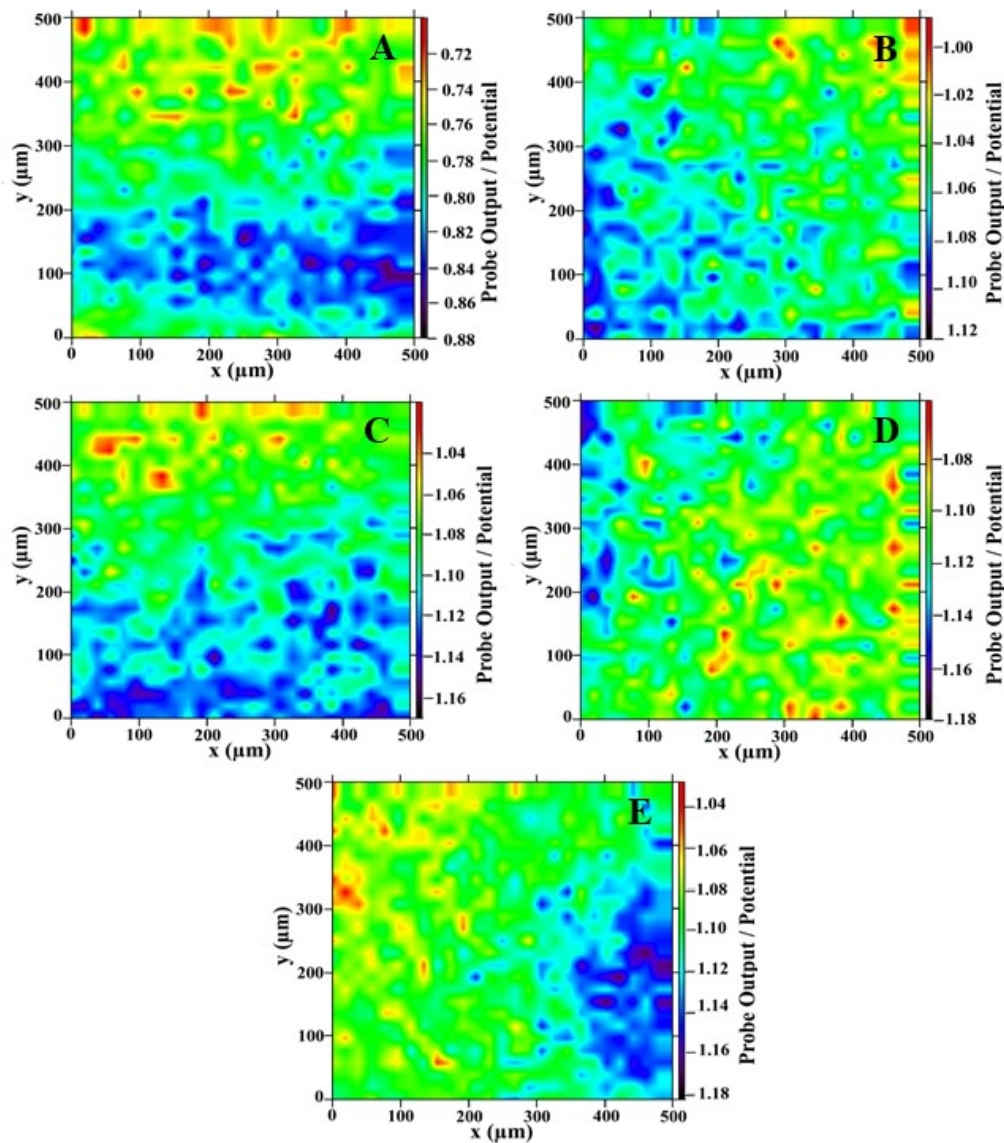


Fig. S14. 2D SKPM images of zinc phosphate coating developed from the bath containing different contents of BVZ composite; (A) 0 wt.%, (B) 0.05 wt.%, (C) 0.1 wt.%, (D) 0.2 wt.% and (E) 0.5 wt.%

Table S1. Phosphating bath composition

Sl. No.	Chemicals	Composition
1	Phosphoric acid (H_3PO_4)	16 mL/L
2	Zinc Oxide (ZnO)	1.2 g/L
3	Sodium Nitrite ($NaNO_2$)	16 g/L
4	Sodium Fluride (NaF)	2 g/L

Table S2. Comparison of roughness parameters of bare zinc phosphate coating and zinc phosphate coatings developed from the containing different amounts of BVZ composite

Coatings	S_a (μm)	S_q (μm)	S_p (μm)	S_v (μm)	S_t (μm)	S_{sk} (μm)	S_{ku} (μm)
Bare ZP	2.879	3.558	16.271	-9.342	25.613	-1.450	3.028
ZP + 0.05 wt.% BVZ	2.795	3.440	10.354	-10.882	21.236	-2.795	2.792
ZP + 0.1 wt.% BVZ	2.527	3.089	9.893	-6.981	16.874	-4.856	2.982
ZP + 0.2 wt.% BVZ	1.593	1.996	5.878	-6.061	11.949	-5.896	3.445
ZP + 0.5 wt.% BVZ	2.122	2.640	8.077	-8.936	17.014	-3.328	3.177

Table S3. Comparison of NIR reflectance and NIR solar reflectance of optimized BVZ composite incorporated zinc phosphate coating after exposure in different solutions

5% Chemicals	NIR reflectance at 1100 nm (R%)	NIR solar reflectance (R*%)
NaCl	45.02	53.90
NaOH	42.18	51.45
HCl	39.25	49.45
HNO ₃	37.69	47.87

Table S4. Comparison of NIR reflectance and NIR solar reflectance of optimized BVZ composite incorporated zinc phosphate coating after exposure to the natural sunlight

Time duration exposure to sunlight (days)	NIR reflectance at 1100 nm (R%)	NIR solar reflectance (R*%)
0	51.92	58.97
10	51.71	58.77
20	51.60	58.55
30	51.49	58.42
40	51.29	58.27
50	51.22	58.17
60	51.16	58.07

Table S5. Temperature measurements in front and behind the coating surface

Sl. No.	coatings	Front coating temperature (°C)	Back coating temperature (°C)	Temperature difference (°C)
1	Bare ZP coating	62.4	56.1	6.3
2	BVZ zinc phosphate coating	52.6	40.8	11.8

Table S6. Electrochemical impedance parameters: bare zinc phosphate coating and different compositions of BVZ composite-based zinc phosphate coating

Coatings	R _S (Ω cm ²)	Q _C (F)	R _C (Ω cm ²)	Q _{dl} (F)	R _{ct} (Ω cm ²)
Bare ZP	11.60	26.31×10 ⁻⁶	50.53	0.565×10 ⁻³	137.7
ZP + 0.05 wt.% BVZ	11.23	9.85×10 ⁻⁶	47.35	1.555×10 ⁻³	175.3
ZP + 0.1 wt.% BVZ	14.02	20.45×10 ⁻⁶	74.7	1.712×10 ⁻³	341.6
ZP + 0.2 wt.% BVZ	22.16	3.09×10 ⁻⁶	188.2	5.814×10 ⁻⁶	765.4
ZP + 0.5 wt.% BVZ	12.72	6.519×10 ⁻⁶	141.6	1.608×10 ⁻³	647.4

Table S7 Comparision of corrosion resistance and reflectance data with reported data

Material	Reflectance	Corrosion resistance	Reference
LiMg _{0.8} Co _{0.2} PO ₄	67%	R _{ct} = 9.3 × 10 ⁹ Ωcm ²	[1]
NaZn _{0.9} Co _{0.1} PO ₄	64%	R _{ct} = 8.8 × 10 ⁶ Ωcm ²	[2]
Potassium titanate whiskers	48 %	Corrosion Rate = 7.531 × 10 ⁻⁴ mm ⁻¹ day ⁻¹	[3]
Green pigments (Co _x Zn _{1-x} O)	30%	-	[4]
Bi _{1-x} La _x FeO ₃	44.1%	-	[5]
SrCaP	-	Corrosion Rate = 2.79 ± 0.03 mm ⁻¹ day ⁻¹	[6]
BVZ composite	51.97%	Corrosion Rate = 1.099 mm ⁻¹ day ⁻¹	Present study

References

- [1] P.K. Thejus, K.V. Krishnapriya, K.G. Nishanth, NIR reflective, anticorrosive magenta pigment for energy saving sustainable building coatings, *Solar Energy*, 222 (2021) 103-114.
- [2] P.K. Thejus, K.V. Krishnapriya, K.G. Nishanth, A cost-effective intense blue colour inorganic pigment for multifunctional cool roof and anticorrosive coatings, *Solar Energy Materials and Solar Cells*, 219 (2021) 110778.
- [3] W. Wang, Y. Tian, H. Shen, X. Zhang, Modified potassium titanate whiskers for preparation of enhanced corrosion-resistant phosphating conversion coatings with high NIR reflectivity on mild steel, *Journal of Alloys and Compounds*, 955 (2023) 170247.
- [4] J.d.O. Primo, K.W. Borth, D.C. Peron, V.d.C. Teixeira, D. Galante, C. Bittencourt, F.J. Anaissi, Synthesis of green cool pigments (CoxZn1-xO) for application in NIR radiation reflectance, *Journal of Alloys and Compounds*, 780 (2019) 17-24.
- [5] L. Yuan, A. Han, M. Ye, X. Chen, L. Yao, C. Ding, Synthesis and characterization of environmentally benign inorganic pigments with high NIR reflectance: Lanthanum-doped BiFeO₃, *Dyes and Pigments*, 148 (2018) 137-146.
- [6] J.G. Acheson, S. McKillop, J. Ward, A. Roy, Z. Xu, A.R. Boyd, P. Lemoine, P.N. Kumta, J. Sankar, B.J. Meenan, Effects of strontium-substitution in sputter deposited calcium phosphate coatings on the rate of corrosion of magnesium alloys, *Surface and Coatings Technology*, 421 (2021) 127446.